

# Preliminary Results of the Alpine Experiment DISKUS

Joerg M. Hacker, Meteorologisches Institut der Universität Bonn.

Presented at the XVII. OSTIV-Congress, Paderborn (F.R.G.), 1981.

During August 1980 the Alpine Experiment DISKUS (*Dischmatal-Klima-Untersuchung*) took place in a region between Davos and St. Moritz in Switzerland. The main purpose of DISKUS was the investigation of the valley wind circulation of the Dischmatal. One of the subprograms was to investigate the influence of the complex topography on the structure of the convection and the turbulent energy fluxes over the experimental area. For this subprogram measurements were made, using three instrumented powered gliders (ASK-16) of the Institut für Physik der Atmosphäre of the DFVLR (Deutsche Forschungs- und Versuchsanstalt für Luft- und Raumfahrt).

**Flight patterns:** As the topography of the DISKUS-area is very nonhomogeneous, two different flight patterns were chosen. Flight pattern I, called "ridge-crossing", consisted of simultaneous flights of the three powered gliders normal to four

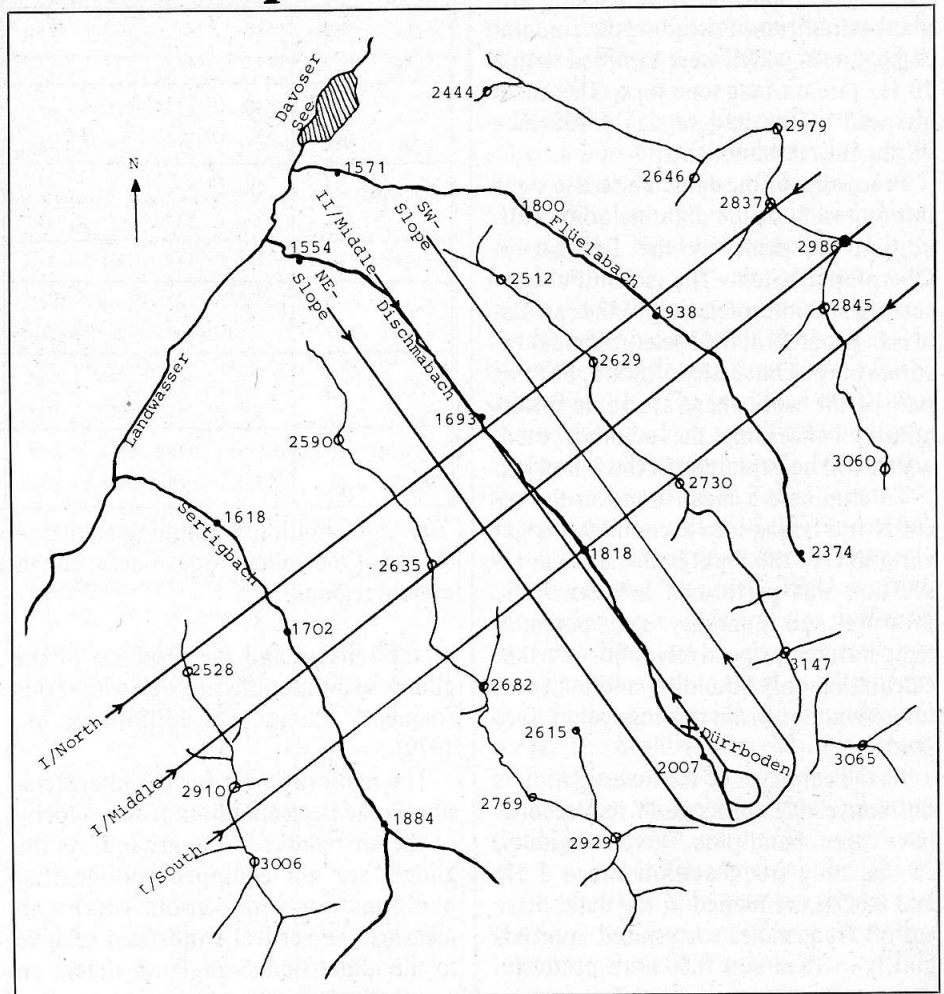


Fig. 1: Sketch of the DISKUS-area with the two flight patterns and the location of the energy balance station Dürrboden.

quasiparallel ridges with three valleys in between (Sertigtal, Dischmatal, Flüelatal). The traverses were performed in 2.5

km horizontal separation and about 200 m above the ridges and 900 to 1200 m above the valley bottoms. The crossing times of the ridges and of the middles of the valleys were marked in the records of the flights.

Flight pattern II, called "valley up and down", consisted of simultaneous flights of two powered gliders up and down the Dischmatal valley about 500 m to 200 m above the valley bottom, one glider flying above the middle of the valley, the other one as near as possible (20-30 m) to one of the slopes at the same altitude. A schematic view of the DISKUS-area is given in Fig. 1. Also shown there are the tracks of the two flight patterns.

**Instrumentation:** The powered gliders are instrumented with a temperature sensor (Pt 100, reverse flow probe), two independent humidity sensors

Date: 10 August 1980 Time: 10.45 - 11.10 GMT Mean height: 2300 m MSL	Standarddeviation			Correlationcoefficient			Mean Flux	
	w	q	0	q/w	0/w	q/0	E W/m <sup>2</sup>	H W/m <sup>2</sup>
	m/s	g/kg	K					
1427A.R05 Middle	0.49	0.087	0.040	0.00	0.01	-0.36	-0.3	0.5
1510A.R05 NE-Slope	1.06	0.275	0.108	0.56	0.20	0.41	407.7	20.1
1427A.R06 Middle	0.70	0.098	0.025	0.05	-0.11	-0.36	9.1	-1.8
1510A.R06 SW-Slope	1.01	0.285	0.083	0.52	0.53	0.62	408.9	44.1
1427A.R07 Middle	0.66	0.112	0.044	-0.12	-0.23	-0.42	-22.1	-6.2
1510A.R07 NE-Slope	1.02	0.204	0.116	0.36	0.26	0.49	186.4	28.0
1427A.R08 Middle	0.75	0.106	0.032	0.21	-0.01	-0.18	41.2	-0.2
1510A.R08 SW-Slope	1.16	0.188	0.096	0.51	0.38	0.35	279.0	38.4
1427A.R05-R08 Middle							7.0	-1.9
1510A.R05-R08 Slopes							320.5	32.7
Dürrboden Energy balance surface (11.00-11.30 GMT, 2000 m MSL)							346.3	162.8

Tab. 1: Statistics of the flights of pattern II. The location of the station Dürrboden, where the surface energy balance has been measured, is marked in Fig. 1.

(Lyman-alpha, Vaisala Humicap), sensors for static and dynamic pressure, vertical velocity and the other relevant airplane parameters as heading etc., in total 16 channels, which were sampled with a 10 Hz rate on magnetic tape. The mean airspeed of the gliders was 35-37 m/s during the measurements.

**Processing of the data:** The basic steps in processing of the data including calibration are done by the DFVLR in Oberpfaffenhofen. The scientific processing and interpretation of the raw data is in progress at the Meteorological Institute of the University of Bonn. For this part of the work there are some uncertainties concerning the methods used, which will be explained in the following.

To eliminate a mean trend in the records and taking into account the height variations of the flight paths, a linear regression was performed between static pressure and humidity and potential temperature respectively. For further calculation only humidity- and temperature-deviations from this regression were used.

As the emphasis of the investigation is on convective processes, the records have been band-pass-filtered digitally, so that only frequencies between 2 Hz and 0.02 Hz remained in the data; these cut-off frequencies correspond approximately to 18 m and 1800 m respectively. The remaining range was defined as the "convective scale". The response times

1510A		RO5	RO6	RO7	RO8	RO5	RO6	RO7	RO8	RO5-RO8	RO5-RO8
Indicator		w	w	w	w	q	q	q	q	w	q
$E_{act}$	$W/m^2$	628	727	303	533	665	718	664	585	548	583
$E_{env}$	$W/m^2$	282	252	120	147	263	254	82	139	200	185
$H_{act}$	$W/m^2$	44	83	55	80	63	85	63	89	66	75
$H_{env}$	$W/m^2$	9	31	16	22	-2	29	12	20	19	15
$E_{act}$	%	58	60	60	67	60	60	73	67	61	65
$H_{act}$	%	75	59	66	67	105	60	76	68	67	77
$Area_{act}$	%	37	34	37	35	37	34	37	32	36	35
$w_{act}$	m/s	1.22	1.22	1.18	1.27	.74	.68	.54	.72		
$w_{env}$	m/s	-.53	-.59	-.52	-.61	-.23	-.31	-.15	-.26		
$q_{act}$	g/kg	.158	.167	.080	.108	.285	.293	.201	.208		
$q_{env}$	g/kg	-.100	-.091	-.060	-.049	-.173	-.158	-.136	-.094		
$\theta_{act}$	K	.013	.045	.028	.039	.050	.047	.061	.028		
$\theta_{env}$	K	-.023	-.028	-.026	-.030	-.045	-.030	-.045	-.021		

Tab. 2: Conditional sampling statistics of the runs 5 to 8 of flight 1510A along the slopes of the valley. Index «act»: convectively active regions; index «env»: environmental regions.

of the sensors and the response of the gliders to air motions are well within this frequency range (e.g. Milford et al., 1979).

The main problem for the interpretation is the determination of the velocity of the air relative to the ground. As the gliders are not equipped with inertial platforms nor with sensors which can measure the vertical windspeed relative to the glider or the angle of attack, an aerodynamic approach must be used to calculate the components of the air mo-

tion relative to the ground. No attempt was made to determine the horizontal component of the wind. The vertical wind component was calculated using an algorithm after Duncan (1952), which was first used for meteorological purposes by Bunker (1955). More recently Fortak (1980) used this approach for similar data sets. The inputs for this method are the vertical velocity of the airplane, the vertical acceleration, the pitch angle, the true air speed and several aircraft parameters such as lift coefficient,

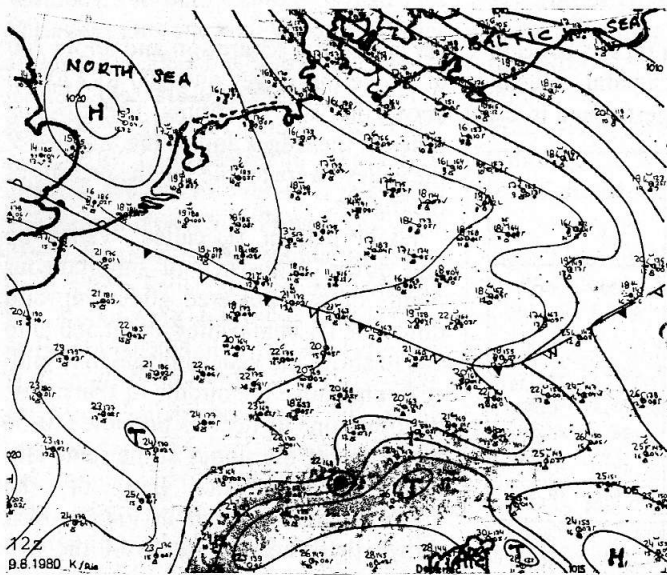


Fig. 2 A: Synoptic situation of 9 Aug. 1980, 12 GMT. The DIS-KUS-area is marked thus ●.

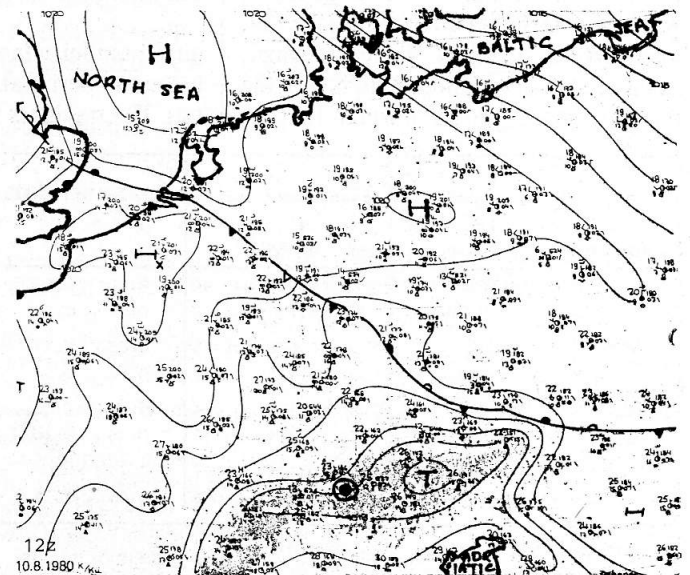


Fig. 2 B: Synoptic situation of 10 Aug. 1980, 12 GMT. The DIS-KUS-area is marked thus ●.

	Mean Heading	Standard deviation			Correlation coefficient			Mean Flux	
		w m/s	q g/kg	Θ K	q/w	Θ/w	q/Θ	E W/m <sup>2</sup>	H W/m <sup>2</sup>
1310A.R01	55	0.46	0.147	0.041	0.26	0.10	-0.37	42	2
R02	235	0.54	0.153	0.055	0.28	0.19	-0.32	53	7
R03	55	0.80	0.184	0.045	0.13	0.03	-0.59	47	2
R04	235	0.79	0.203	0.070	0.22	0.20	-0.18	84	11
R05	55	0.73	0.163	0.046	0.19	0.25	-0.37	57	8
R06	235	0.75	0.177	0.055	0.18	-0.10	-0.45	57	-4
R07	55	0.82	0.209	0.056	0.22	0.08	-0.45	95	4
R08	235	0.47	0.201	0.046	0.12	-0.13	-0.59	31	-3
1426A.R01	55	0.85	0.146	0.067	0.23	-0.10	-0.36	74	-6
R02	235	0.83	0.144	0.064	0.40	0.19	0.32	120	10
R03	55	0.93	0.142	0.048	0.11	0.16	-0.03	35	7
R04	235	0.79	0.166	0.050	0.18	0.01	-0.37	58	1
R05	55	0.77	0.172	0.058	0.12	-0.05	-0.40	38	-2
R06	235	0.89	0.125	0.051	0.35	0.02	-0.17	96	1
R07	55	0.83	0.154	0.041	0.17	-0.07	-0.44	55	-3
R08	235	0.90	0.220	0.063	0.26	-0.18	-0.46	126	-10
1508A.R01	55	0.70	0.114	0.053	0.28	-0.20	-0.20	56	-7
R02	235	0.75	0.089	0.048	0.13	0.04	-0.04	21	2
R03	55	0.70	0.147	0.052	0.06	-0.11	-0.28	15	-4
R04	235	0.67	0.139	0.055	0.13	0.07	-0.22	30	2
R05	55	0.79	0.167	0.058	0.24	0.09	-0.24	77	4
R06	235	0.75	0.134	0.054	0.17	0.07	-0.17	41	3
R07	55	0.82	0.138	0.057	0.27	0.00	-0.15	77	-0
R08	235	0.62	0.113	0.065	0.08	0.05	0.20	14	2
1311B.R09	55	0.67	0.253	0.052	0.14	0.03	-0.61	60	1
R10	235	0.78	0.283	0.071	0.18	-0.16	-0.67	101	-9
R11	55	0.74	0.276	0.041	0.27	-0.13	-0.39	139	-4
R12	235	0.86	0.336	0.065	0.13	-0.02	-0.52	96	-1
1427B.R09	55	1.01	0.193	0.042	0.31	-0.08	-0.12	152	-4
R10	235	0.83	0.216	0.053	0.20	-0.01	-0.33	88	-1
R11	55	0.96	0.212	0.055	0.25	0.12	-0.38	126	6
R12	235	0.84	0.312	0.053	0.36	-0.16	-0.66	238	-7
1510B.R09	55	0.92	0.119	0.058	0.43	0.21	-0.08	118	12
R10	235	0.85	0.166	0.055	0.41	0.00	-0.11	146	0
R11	55	0.96	0.192	0.041	0.32	0.07	-0.06	145	3
R12	235	1.01	0.187	0.052	0.21	0.18	-0.08	98	10

Tab. 3: Statistics of the flights of pattern I.

weight, etc. A detailed description of the method of computation is given in the above cited papers. During this work it became obvious that further testing of the method is necessary and this is the main reason for any uncertainties in the results.

44 runs were processed as described in this chapter. From these runs mean values, standard deviations, covariances and energy fluxes were computed. Additionally powerspectral densities for some parameters were estimated. Finally the

conditional sampling technique was used to compare statistics for convectively active regions of the runs statistics for the environment.

**Synoptic situation:** The flights were made on 9 and 10 August 1980. The synoptic situations of these days are shown in Fig. 2A and 2B respectively. The boundary layer was capped by a subsidence inversion at about 3100-3200 m above sea level. On 9 August 2/8 to 4/8 orographic cumulus developed with bases at about 3000 m. On 10 August no

clouds developed along the flight tracks. The mesoscale winds were weak with a main component normal to the ridges. The mean height of the traverses across the ridges was 2900 m on 9 August and 3000 m on 10 August.

**Results of flight pattern II:** Fig. 3A shows a portion of a flight near the NW slope of the valley on 10 August, 10.45 GMT. The prominent features are the sharp-edged bursts of temperature and humidity, which are well correlated with increased turbulence and ascending air. On the other hand the air above the middle of the valley at the same time is fairly calm (Fig. 3B). The standard deviations of vertical wind  $w$ , specific humidity  $q$  and potential temperature  $\Theta$  for the different runs are given in Tab. 1. There are also given the correlation coefficients between these three parameters. As expected, there is a relatively high positive correlation between  $w$  and  $q$  as well as  $\Theta$  near the slopes and nearly no correlation in the middle of the valley. This seems to be more pronounced in the humidity records. The negative correlation between  $q$  and  $\Theta$  in the middle of the valley may be an effect of the weak compensating sinking of warm and dry air, which ascends warm and moist along the slopes.

For the four runs near the slopes and the four runs in the middle of the valley turbulent fluxes of latent and sensible energy ( $E$  and  $H$ ) have been computed, using the direct eddy-correlation method. Time series of the instantaneous values of the fluxes (covariances) are included in Fig. 3, and the mean fluxes in Tab. 1. For comparison the estimates of the fluxes at the surface as determined by the energy balance method of Kerschgens (personal communication) are also given. The flux of latent energy near the slopes agrees very well with this independent estimate; the difference in the fluxes of sensible energy may be explained with the well known fact that this flux decreases more rapidly with height than the flux of latent energy (e.g. Milford et al., 1979).

Fig. 4 shows the mean powerspectral densities of vertical velocity, specific humidity and potential temperature for the four runs near the slopes of the valley. The spectral densities have been estimated for 1024 frequencies using the fast

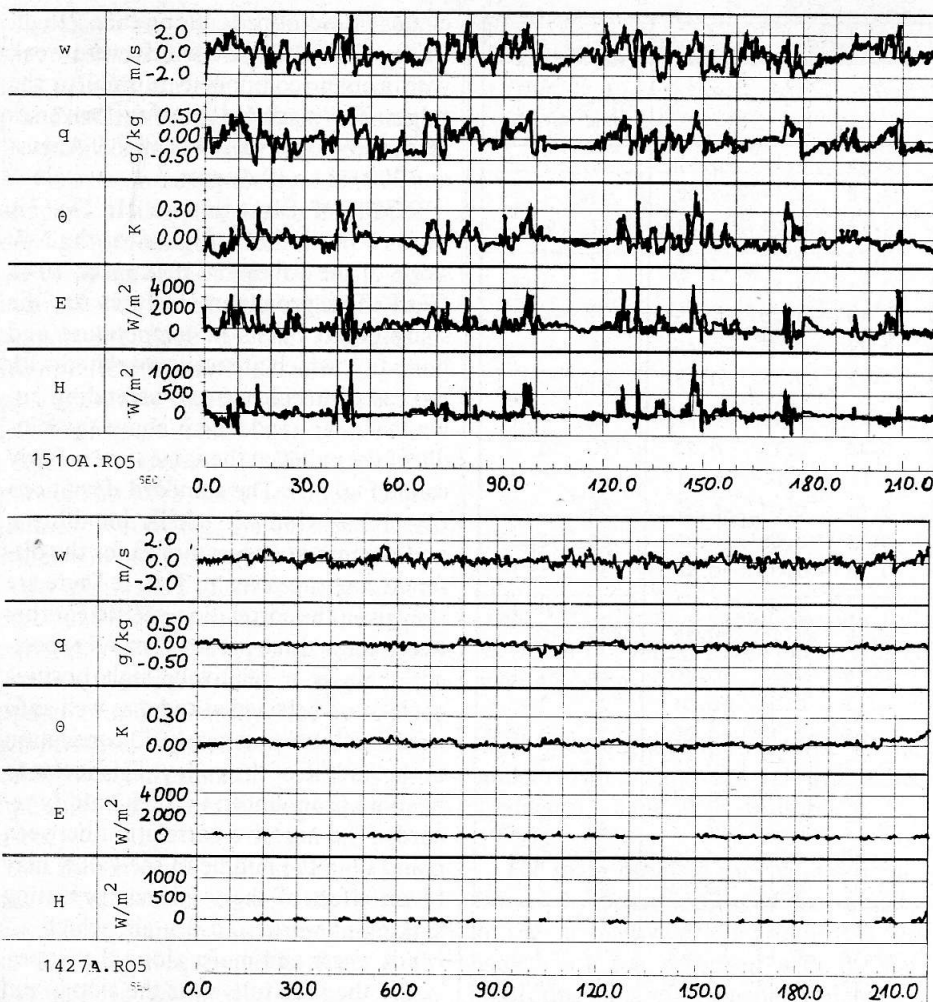


Fig. 3: Time series of vertical velocity  $w$ , specific humidity  $q$ , potential temperature  $\Theta$ , and the instantaneous values of the fluxes (covariances) of latent ( $E$ ) and sensible ( $H$ ) energy for two flights of pattern II. Upper: Flight 1510A, Run 5, along the NE-slope; lower: Flight 1427A, Run 5, over the middle of the valley.

Fourier transform algorithm and are smoothed over 10% of the respective wavelengths. The wavelength is approximated by  $\lambda = \text{TAS} / \nu$ , where TAS equals the mean true air speed of the runs (36 m/s). The slope of the spectra is in good agreement with the  $-5/3$  law (straight line).

For the same runs conditional sampling techniques were tried for distinguishing between convectively active regions of the flights and the environment. As indicator functions, vertical velocity and specific humidity were used to give two independent estimates. The condition for convective regions was  $w > \bar{w} + 0.25\sigma_w$  for at least three data points, which corresponds to a minimum burst-length of 15 m. In the case where specific humidity was used as indicator function

an adequate condition was used. The results for the four runs and the two different indicator functions are summed in Tab. 2. For both cases the energy fluxes in the active regions are with one exception about three to five times the fluxes in the environment. The active area consists of 32% to 37% of the total area and contributes 58% to 73% to the total flux. Typical deviations of vertical velocity, specific humidity and potential temperature from their mean values are also given in Tab. 2. The deviations for the active regions are about twice the values for the environment, which seems to be reasonable, because the forcing of the convective processes is the warm and moist ascending air, while the sinking of dry and cold air is mainly a compensating process. The mean burstlengths are 56 m for

the  $w$ -bursts and 50 m for the  $q$ -bursts. Manton (1977) found a similar length scale for temperature bursts in 100 m above the ground in Australia. A histogram of the mean burstlengths is shown in Fig. 5.

**Results of flight pattern I:** During the two days 36 traverses across the ridges were flown. The flights were made just below the inversion, which was topped with 4/8 cumulus on 9 August and without any clouds on 10 August. The records of three simultaneous NE-SW-runs are shown in Fig. 6. The records start in the middle of the Flüelatal and end in the middle of the Sertigtal. The differences in the intensity of the humidity-, temperature- and vertical velocity-fluctuations between the air over the ridges and the air over the valleys can clearly be seen. Even more striking are the peaks of the instantaneous values of the fluxes (covariances)  $\rho_c w' \Theta'$  and  $\rho L w' q'$ , which appear only in the vicinity of the ridges. Another feature of the records is the positive correlation between  $q$  and  $\Theta$  around the ridge at the SW-slope of the Dischmatal, while this correlation is more negative at the NE-slope. Perhaps this is an effect of the slightly different insolation of the two slopes or of different types of soil and vegetation.

Tab. 3 shows that vertical velocity and specific humidity are positively correlated, but the correlation coefficient has only values of about 0.2. The correlation between vertical velocity and potential temperature becomes insignificant for most of the runs and changes sometimes to negative values. These correlations show that the flux of latent energy is the dominant process, while the flux of sensible energy is small and has a tendency to negative values. Throughout nearly all runs there is a negative correlation be-

Dimension: $W/m^2$		Mean Fluxes		rms-Variability	
		E	H	E	H
1310A.R01-R08	North	58.2	3.4	21.4	5.3
1427A.R01-R08	Middle	75.3	0.3	35.3	6.7
1508A.R01-R08	South	41.4	0.2	25.9	3.9
1311B.R09-R12	North	98.8	-3.0	32.2	4.0
1427B.R09-R12	Middle	151.1	-1.2	63.7	5.7
1510B.R09-R12	South	126.7	6.1	23.4	5.3

Tab. 4: Mean energy fluxes and their variability for the flights of pattern I.

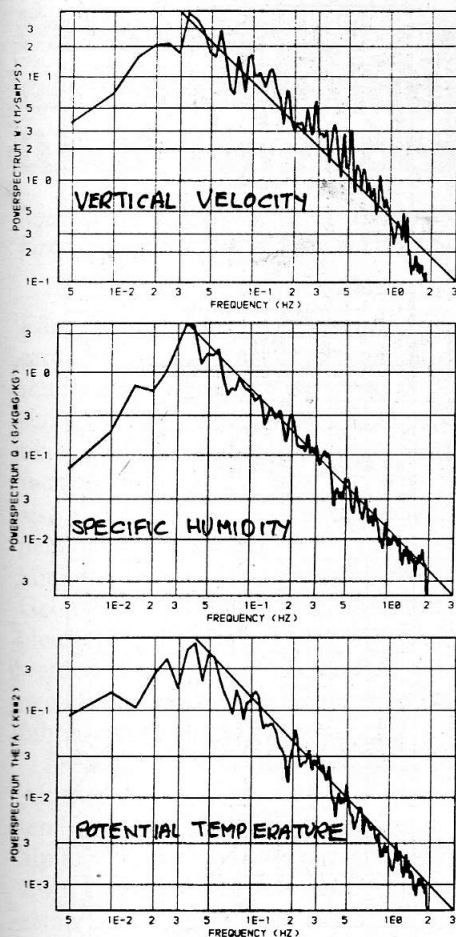


Fig. 4: Mean powerspectral densities of vertical velocity  $w$  (upper), specific humidity  $q$  (middle) and potential temperature  $\Theta$  (lower) for the runs of flight 1510A along the slopes of the valley. The spectral estimates are smoothed over 10% of the respective wavelengths, the straight lines have a slope of  $-5/3$ .

tween specific humidity and potential temperature, which means, that the ascending moist air is mostly colder than the environment. Similar results have been found by Wyngaard et al (1978) in the upper part of the mixed layer for the AMTEX-area. The strongest negative correlations are found in the northernmost traverses (flights 1310A/1311B), which have the greatest mean height above the ground.

The fluxes of latent heat on 10 August are two to three times larger than the fluxes on 9 August (Tab. 4). This can be explained by the maximum of insolation and evaporation at about 11.30 to 12.00 GMT (Kerschgens, personal communication), which means that the flights on

10 August fell in the build up phase and the maximum of the convection, while the flights on 9 August are made during decreasing convection. Additionally listed in Tab. 4 is the rms-variability (standard deviation) of the fluxes between the runs; a typical value of this variability is about 50% of the mean flux. A part of this variability may be due to the uncertainties, which are contained in the computation of the vertical velocity.

The mean powerspectral densities of vertical velocity (Fig. 7) show, that the variance of  $w$  is produced by two different length scales, which are separated by a spectral gap. The smaller scale reaches from the turbulent processes up to about 180 m (0.2 Hz), the scale of the small thermals, which were intersected during the crossing of the ridges near the ground. The peaks in the larger scale are found between 600 m and 900 m (0.06 Hz-0.04 Hz) and belong to the organized

convection cells over the slopes. The separation between the two scales is best pronounced in the northernmost flights. The reason may be, that the small thermals there had more time (height) to organize than at the other traverses, which were in the mean flown nearer to the ground.

As for the flights of pattern II it was also tried to distinguish between convectively active and environmental regions of the rms, but here only vertical velocity was used as indicator function for convection. The results are presented in Tab. 5. For all runs 36% to 37% of the total area contributes 63% to 86% of the total flux of latent energy. This means, that the ratio between the typical fluxes for the active regions and for the environment is of the order of 3 to 10. For the runs of flight pattern II near the slopes a ratio of 1.5 to 3 was found. This difference may be explained as follows: the en-

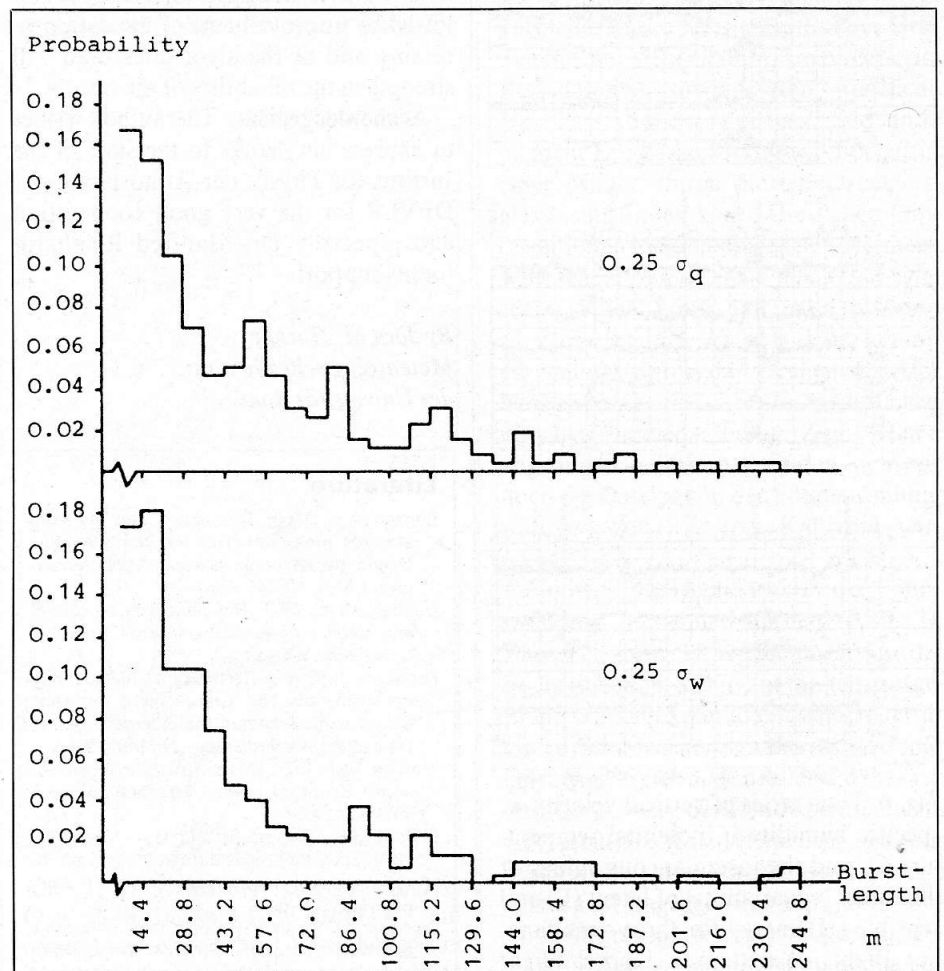


Fig. 5.: Histograms of the burstlengths of velocity  $w$  (lower) for the runs of flight specific humidity  $q$  (upper) and vertical 1510A along the slopes of the valley.

	1310A RO1-RO8	1426A RO1-RO8	1508A RO1-RO8	1311B RO9-R12	1427B RO9-R12	1510B RO9-R12
$E_{act}$ $W/m^2$	136	149	70	189	259	233
$E_{env}$ $W/m^2$	15	36	25	49	89	71
$E_{act}$ %	86	70	65	71	63	67
$Area_{act}$ %	37	36	38	37	37	36

Tab. 5: Conditional sampling statistics of the flights of pattern I.

Environmental portions of the runs near the slopes consist of relatively strong compensating downdrafts, which are dry and cold, and therefore contribute significantly to the upward energy flux. The environmental regions of the runs across the ridges, on the other hand, are found mainly between the ridges, in the relatively calm air over the valleys.

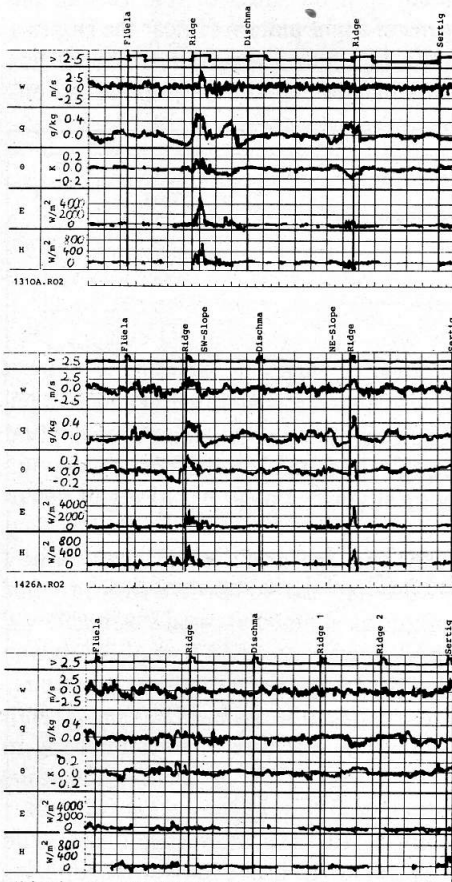


Fig. 6: Time series of vertical velocity  $w$ , specific humidity  $q$ , potential temperature  $\Theta$ , and the instantaneous values of the fluxes (covariances) of latent ( $E$ ) and sensible ( $H$ ) energy for three simultaneous flights of pattern I. Upper: Flight 1310A, Run 2; middle: Flight 1426A, Run 2; lower: Flight 1508A, Run 2.

**Conclusion:** It has been demonstrated that powered gliders are a useful tool in investigating the planetary boundary layer. Some of the results, especially those of the runs of flight pattern II could hardly be achieved by any other instrumented platform, because only the high manoeuvrability of the powered gliders enables them to fly as near the ground as is necessary. Although there remain some uncertainties in the results, it can be stated that the meteorological findings of the investigation are reasonable. Further testing, which will be followed by improvements of the data processing and of the algorithms used will strengthen the reliability of the results.

**Acknowledgement:** The author wishes to express his thanks to the staff of the Institut für Physik der Atmosphäre der DFVLR for the very good cooperation and especially Dr. Manfred Reinhardt for his support.

By Jörg M. Hacker,  
Meteorologisches Institut  
der Universität Bonn

### Literature

- Bunker, A.F., 1955: Turbulence and shearing stresses measured over the North Atlantic Ocean by an airplane-acceleration technique. *J. Met.*, 12, 445-455.
- Duncan, W.J., 1952: The principles of control and stability of aircraft. London, Cambridge Univ. Press, 384pp.
- Fortak, H., 1980: Messtechnische Untersuchung der planetarischen Grenzschicht mit Hilfe eines instrumentierten Motorseglers. *Ber. d. Deutschen Wetterdienstes*, Nr. 149, 166 pp.
- Manton, M.J., 1977: On the structure of convection. *Boundary-Layer Meteorology*, 12, 491-503.
- Milford, J.R., S. Abdulla and D.A. Mansfield, 1979: Eddy flux measurements using an instrumented powered glider. *Quart. J.R. Met. Soc.*, 105, 673-693.
- Wyngaard, J.C., W.T. Pennell, D.H. Lenschow and M.A. LeMone, 1978: The temperature-humidity covariance budget in the convective boundary layer. *J. Atmos. Sci.*, 35, 47-58.

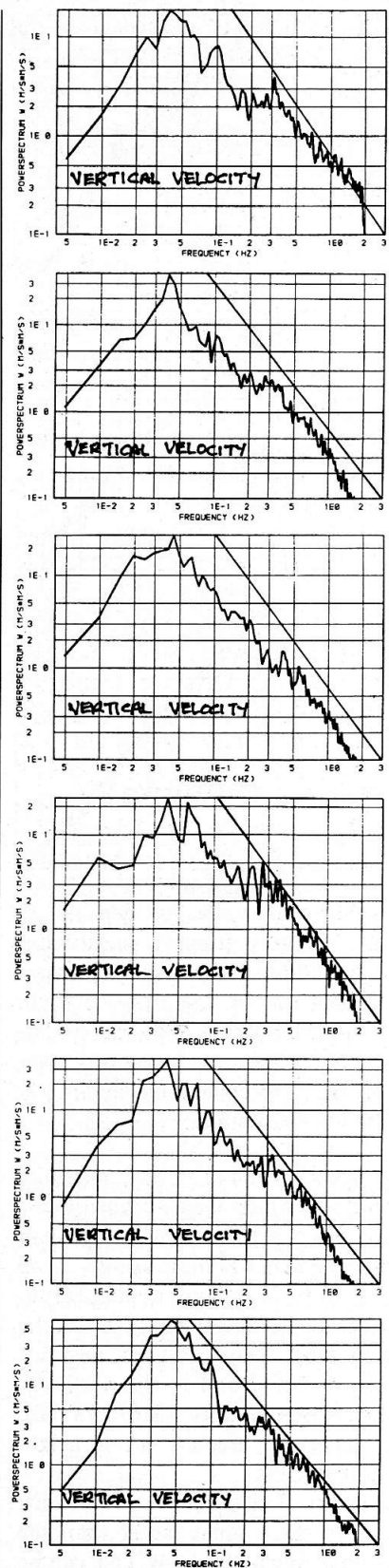


Fig. 7: Mean powerspectral densities of vertical velocity  $w$  for the flights of pattern I.